

1 **Nature lessons: the whitefly bacterial endosymbiont is a minimal amino acid factory**  
2 **with unusual energetics**

3

4 Jorge Calle-Espinosa<sup>1</sup>, Miguel Ponce-de-Leon<sup>1</sup>, Diego Santos-Garcia<sup>2,3</sup>, Francisco J. Silva<sup>2,4</sup>,  
5 Francisco Montero<sup>1\*</sup> & Juli Peretó<sup>2,5\*</sup>

6 \*Corresponding authors: Francisco Montero [framonte@quim.ucm.es](mailto:framonte@quim.ucm.es) - Juli Peretó

7 [Juli.Pereto@uv.es](mailto:Juli.Pereto@uv.es)

8 <sup>1</sup>Departamento de Bioquímica y Biología Molecular I, Facultad de Ciencias Químicas,  
9 Universidad Complutense de Madrid, Ciudad Universitaria, Madrid 28045, Spain.

10 <sup>2</sup>Institut Cavanilles de Biodiversitat i Biologia Evolutiva, Universitat de València, C/José  
11 Beltrán 2, Paterna 46980, Spain.

12 <sup>3</sup>Present address: Department of Entomology, The Hebrew University of Jerusalem, Israel.

13 <sup>4</sup>Departament de Genètica, Universitat de València.

14 <sup>5</sup>Departament de Bioquímica i Biologia Molecular, Universitat de València.

15

16 **Abstract**

17

18 Bacterial lineages that establish obligate symbiotic associations with insect hosts are  
19 known to possess highly reduced genomes with streamlined metabolic functions that are  
20 commonly focused on amino acid and vitamin synthesis. We constructed a genome-scale  
21 metabolic model of the whitefly bacterial endosymbiont *Candidatus Portiera aleyrodidarum*  
22 to study the energy production capabilities using stoichiometric analysis. Strikingly, the  
23 results suggest that the energetic metabolism of the bacterial endosymbiont relies on the use  
24 of pathways related to the synthesis of amino acids and carotenoids. A deeper insight showed  
25 that the ATP production via carotenoid synthesis may also have a potential role in the

26 regulation of amino acid production. The coupling of energy production to anabolism suggest  
27 that minimization of metabolic networks as a consequence of genome size reduction does not  
28 necessarily limit the biosynthetic potential of obligate endosymbionts.

29

### 30 **Keywords**

31 *Portiera aleyrodidarum*, elementary flux modes, essential amino acids, carotenoids

32

33       Nutritionally driven symbioses between insects and one or more intracellular,  
34 maternally inherited bacteria (endosymbionts) are widespread(1). These mutualistic  
35 associations allow insects to colonize novel ecological niches with unbalanced nutritional  
36 sources. The extreme difficulty to culture obligate endosymbionts outside of their hosts has  
37 limited the study of the interactions between symbionts and hosts mainly by using  
38 comparative genomics(2). Obligate endosymbionts usually have highly reduced genomes  
39 (<1,000 kb), which contain a conserved core of housekeeping genes, and genes for the  
40 biosynthesis of amino acids and vitamins that are essential for the host(1). The synthesis of  
41 these essential compounds requires, in many cases, the metabolic complementation with the  
42 host or from other coexisting endosymbionts(3). Although the nutritional role of obligate  
43 endosymbionts is well defined, other important aspects of the endosymbiont's biochemistry  
44 are less known. In spite of the fact that the metabolic networks of endosymbionts are  
45 relatively small, they are significantly complex and systems biology approaches are needed to  
46 further understand the physiology of these microorganisms. Earlier research approaches used  
47 techniques derived from graph theory and stoichiometric analysis. In particular, these  
48 techniques have been used to infer plausible scenarios of metabolic complementation(4–8), to  
49 determine the fragilities of the metabolic networks(5–8), to reveal characteristics of the transit

50 from free-life to endosymbiosis(5, 8) and to further understanding of nitrogen management in  
51 these systems(5, 7).

52

53 However, to the best of our knowledge, it is still unclear to which extent endosymbionts are  
54 dependent upon their hosts for the necessary energy to support cellular processes and no  
55 previous work (neither theoretical nor experimental) has focused on this aspect of the  
56 endosymbiont's biology. Specifically, can these bacteria be energetically independent from  
57 their host? And, if this is the case, how do they operate to perform such a task? The answer to  
58 these questions is important not only for an understanding of insect-bacteria symbiosis, but  
59 also in order to set the limits of genome reduction properly, a matter of major importance in  
60 fields such as synthetic biology.

61

62 Among the known endosymbionts, *Candidatus Portiera aleyrodidarum* (hereafter  
63 referred to as *Portiera*), hosted in the whitefly bacteriocyte(9), displays a key characteristic  
64 that make it a good candidate for a study in this direction: it contains the set of genes coding  
65 for cytochrome oxidase, NADH dehydrogenase, and ATP synthase, and has the most reduced  
66 genome among endosymbionts with these traits(10). This feature suggests that potentially  
67 *Portiera* is energetically autonomous even though the endosymbiont metabolic network, in  
68 obligate cooperation with the host, is involved in the synthesis of essential amino acids and  
69 carotenoids(11–15). The results presented in this paper support the hypothesis that *Portiera* is  
70 capable of synthesized its own ATP from the resources provided by the whitefly, due to the  
71 utilization of a limited number of pathways related to the synthesis of well-defined amino  
72 acids and/or carotenoids. Moreover, the involvement of the carotenoid synthesis in ATP  
73 production suggests that this pathway is a potential point for the insect to regulate amino acid

74 production. Thus, the characterization of *Portiera*'s metabolism demonstrates the richness of  
75 the energetics of endosymbionts.

76

## 77 **Background**

78 The structure of any metabolic network can be represented by its corresponding  
79 stoichiometric matrix  $N_{m \times n}$ , where each element  $n_{ij}$  corresponds to the stoichiometric  
80 coefficient of metabolite  $i$  in reaction  $j$ . Hereafter, along with  $N_{m \times n}$  several constraints are  
81 needed to properly assess the properties of the associated metabolic network: the  
82 thermodynamic constraints, which prevents the irreversible reactions from taking negative  
83 flux values; the lower and upper bounds imposed over each reaction flux to represent specific  
84 environments (e.g. amount of available nutrients) or enzymatic/transporter maximum  
85 capacities; and the specific kinetic laws that govern each reaction of the network.

86 Unfortunately, the above-mentioned kinetic laws are often unknown. However, metabolism is  
87 characterized by usually fast reactions and high turnover of metabolites when compared to  
88 regulatory events and thus, a pseudo-stationary state (*i.e.* the metabolite concentrations are  
89 assumed constant) can be assumed as an approximation. Taking all restrictions into account,  
90 the set of all possible flux distributions (*i.e.* vector of reaction fluxes), the so-called flux space  
91 (F), is defined as follows:

$$92 \quad F = \left\{ \vec{v} \in \mathbb{R}^n : N \cdot \vec{v} = d\vec{c}/dt = 0, \beta_i \leq v_j \leq \alpha_i \forall j \in J, \beta_i = 0 \forall i \in Irr \right\} \quad (1)$$

93 where  $v$  is the flux distribution,  $c$  is the vector of metabolite concentrations,  $\beta_i$  and  $\alpha_i$   
94 correspond to the lower and upper bound of reaction  $i$ , respectively; and  $Irr$  is the set of the  
95 irreversible reaction indexes.

96

97 Elementary flux modes (EFM) are a special set of flux distributions which fulfills the  
98 constraints in equation (1) and is non-decomposable, that is, no reaction can be deleted from  
99 an EFM and still obtain a valid (non-trivial) steady-state flux distribution. The most  
100 interesting property of these EFMs is that their combinations (convex or linear depending on  
101 the existence of irreversibilities) can generate the complete flux space. Attending to this, the  
102 shared properties of the set of EFMs can be extrapolated to every possible flux distribution  
103 and thus, a proper analysis of these EFMs can lead to a better understanding of the capabilities  
104 of the related metabolic network.

105

## 106 **Results**

### 107 **Genome-scale metabolic reconstruction**

108 Metabolic reconstruction was based on the annotated pan-genome, derived from six  
109 previously published different strains of *Portiera* (ref. 14 and references therein). The pan-  
110 genome contains a total of 280 genes, of which 160 were annotated as enzyme coding genes.  
111 A first draft of the metabolic network was generated using the SEED(16) pipeline. The draft  
112 obtained (id: Seed1206109.3.1165) included 136 internal reactions, 14 exchange fluxes and  
113 one biomass equation. Although the SEED pipeline includes a step for gap-filling the missing  
114 reactions, which are essential for the synthesis of all biomass precursors, the outputted model  
115 was not able to predict biomass formation. Moreover, ~95% of the reactions were found to be  
116 blocked. Thus, in order to obtain a consistent model, a detailed manual curation was  
117 performed using the unconnected modules approach(6) (see Supplementary Appendix 1 for  
118 details).  
119 During the curation a total of 13 enzymatic activities, all related with amino acid biosynthesis

120 and the pentose phosphate pathway (PPP) and coded by 10 genes, mostly contributed by the  
121 host(13–15), were added to the model (Table 1). To assess the essentiality of these orphan  
122 reactions, an *in-silico* knock-out analysis was performed. The result showed that only  
123 ribulose-phosphate 3-epimerase (EC 5.1.3.1) and glucose 6-phosphate isomerase (EC 5.3.1.9)  
124 do not significantly affect the predicted growth (see Supplementary Appendix 1, Figure 10,  
125 Table 1 labelled as \*). In contrast, the synthesis of phosphoenolpyruvate (PEP) depends on  
126 either one of two orphan reactions: PEP synthase (EC 2.7.9.2) or, PEP carboxykinase (EC  
127 4.1.1.49, Table 1 labelled as ^), although the uptake of this metabolite from the host may not  
128 be discarded. Regarding the synthesis of branched chain amino acids, BCA (see  
129 Supplementary Appendix 1, Figures 6 and 7), the behaviour of the model does not change  
130 whether the endosymbiont or the host performs the transamination step. Finally, the last step  
131 of the histidine biosynthesis, catalysed by histidinol dehydrogenase (EC 1.1.1.23), may be  
132 carried by the host even though it is included in the endosymbiont network (see  
133 Supplementary Appendix 1, Figure 2). As a consequence of the manual curation, a flux  
134 consistent (*i.e.* every reaction can carry flux in the stationary state) genome-scale model of  
135 *Portiera*, named *iJC86* predicting biomass formation was obtained (see Supplementary Table  
136 1).

137

### 138 **Assessing the metabolic capabilities of *Portiera***

139 According to *iJC86 in-silico* predictions, *Portiera* is able to produce  $\beta$ -carotene and  
140 nine essential amino acids for the whitefly (see Table 2). Although the majority of enzyme-  
141 coding genes for these pathways have been found in the endosymbiont genome, some of the  
142 reactions are orphans. These orphan reactions include the transamination step at the end of the  
143 BCA biosynthesis, as well as the last two steps in the histidine pathway (Table 1). The

144 stoichiometric analysis of *iJC86* suggested that certain intermediate metabolites of these  
145 pathways must be exchanged between the endosymbiont and its host. In view of these  
146 observations, different scenarios of metabolic complementation are proposed (Figure 1). The  
147 first one is related to the exchange of glutamate and  $\alpha$ -ketoglutarate. The whitefly provides  
148 glutamate to *Portiera*, which spends it on several transamination reactions. The  $\alpha$ -  
149 ketoglutarate produced as a by-product can either be used as a precursor in the lysine  
150 biosynthesis pathway or transported to the insect. A second metabolic complementation event  
151 appears as a consequence of the by-product formation of 5-amino-1-ribofuranosyl-imidazole-  
152 4-carboxamide (AICAR) during histidine biosynthesis. Although AICAR is also a precursor  
153 in the *de novo* synthesis of purine bases, *Portiera* lacks the genes associated with this  
154 pathway. Accordingly, AICAR might be exported to the bacteriocyte cytoplasm, where it  
155 could be used by the host metabolism.

156

157 The synthesis of  $\beta$ -carotene also involves metabolic collaboration between *Portiera* and the  
158 whitefly. According to the model, the biosynthetic precursor geranylgeranyl diphosphate  
159 should be imported from the bacteriocyte and reduced to  $\beta$ -carotene using ubiquinone which  
160 is reoxidized by a membrane-associated ubiquinol oxidase (EC 1.10.3.10), generating a  
161 proton-motive force.

162

163 The last complementation suggested by the model involves the bacteriocyte tricarboxylic acid  
164 (TCA) cycle, a pathway absent in the endosymbiont. In *Portiera*, the synthesis of lysine and  
165 arginine entails the production of succinate and fumarate, respectively. However, since the  
166 endosymbiont lacks any reaction able to consume these compounds, a plausible scenario is  
167 that both metabolites are exported to the bacteriocyte's cytoplasm.

## 168 **Dissecting *Portiera's* energetics through elementary flux modes analysis**

169 One remarkable feature of *Portiera's* metabolism is that it lacks several canonical  
170 energy-conserving pathways, namely, glycolysis, a complete TCA cycle, and fatty-acid  
171 oxidation. Furthermore, only a fragmented PPP, and the production of succinyl-CoA and  
172 acetyl-CoA are retained in the endosymbiont. This striking characteristic is shared with other  
173 endosymbionts of equal or smaller genome size (*e.g. Carsonella, Sulcia, Uzinura, Tremblaya*  
174 *and Hodgkinia*, see(10)). Because *Portiera* can synthesize the same number of amino acids as  
175 endosymbionts with larger genomes, the characterization of its energetics could serve as a  
176 model for the study of the endosymbionts harbouring the most reduced genomes with equal  
177 or more limited biosynthetic capabilities.

178 A detailed study of the energetics of *Portiera* was performed by analysing the elementary flux  
179 modes (EFMs) of the *iJC86* model (see Methods). Briefly, an EM contains a minimal and  
180 unique set of enzymatic reactions that can support cellular functions at steady state and, more  
181 important, any metabolic behaviour under this assumption can be expressed as combination of  
182 these EMs. Thanks to this property, the evaluation of the EFMs associated with the  
183 production of energy, referred to as energy-producing EFMs (enEFMs, see Elementary Flux  
184 Modes Analysis in the Methods section), allows the characterization of every energetic  
185 pathway in the model.

186

187 **Definition I:** *an energetic EFM (enEFM) of a metabolic network is an EFM that produces a*  
188 *net amount of energy in the form of ATP.*

189

190 The *iJC86* model accounts for 6,503 EFMs, of which only 34 are enEFMs. To  
191 completely characterise the energetics associated to these enEFMs, each one was assigned



192 with seven properties: net NADPH production; net NADH production;  $H^+$ gap (net cytosolic  
193  $H^+$  consumption not considering the cytosolic  $H^+$  lost by pumping reactions); ATP consumed;  
194 net ATP production; fraction of produced ATP corresponding to the  $H^+$  gap; and the number  
195 of transported molecules through the membrane (see Supplementary Table 2 for a complete  
196 list of the enEFMs and their properties). The relation between these properties is deduced and  
197 discussed in Supplementary Appendix 2.

198

199       Essentially, every production in the network is either an amino acid or it is linked to  
200 the synthesis of one. Based on this, it is possible to characterize each enEFM through the  
201 assignment of an order, which is defined as follows:

202

203 **Definition II:** the *order* of an enEFM is the number of amino acids that are produced in this  
204 enEFM.

205

206       Furthermore, the amino acids produced by *Portiera* can be classified as follows:

207

208 **Definition III:** an amino acid is energetic if it is produced in an order one enEFM. In  
209 general, a set of amino acids is called energetic if, and only if, no other enEFM produces a  
210 subset of these same amino acids.

211

212 **Definition IV:** an amino acid is defined as energy-dependent if, after discounting the  
213 contribution of the energetic amino acid sets, the amount of energy produced in each  
214 particular enEFM involved is less than zero (energetically self-sufficient if equal to zero).

215

216 It is important to consider that, in general, these definitions hold only if no zero order  
217 enEFMs exist in the model: if the former is not true, it cannot be assured that the energy  
218 produced in enEFM of order  $> 0$  is related to the amino acids synthesized in it. However, the  
219 *iJC86* model has one. This enEFM comprises solely the synthesis of  $\beta$ -carotene from the  
220 geranylgeranyl diphosphate imported from the host (see Supplementary Appendix 1, Figure  
221 15). In this pathway four double bonds are formed, each of which requires the concomitant  
222 reduction of a quinone to quinol. These four quinol molecules are incorporated and  
223 reoxidized in the respiratory chain, and 2.5 molecules of ATP *per*  $\beta$ -carotene synthesized may  
224 be produced. Because no other enEFM is associated with the production of  $\beta$ -carotene, it can  
225 be assumed that definitions III and IV hold even with the presence of this zero order enEFM.  
226 The characteristics of the enEFMs, which only produce energetic amino acid sets, are given in  
227 Table 3, and a representation of the energetics of *Portiera* is displayed in Figure 2.

228

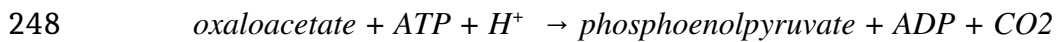
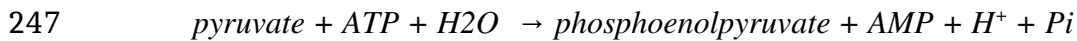
229 While no enEFMs of order one has been found, a total of eleven enEFMs of order two  
230 were identified. These enEFMs involve four distinct pairs of amino acids (see Table 3):  
231 leucine/histidine; valine/histidine; lysine/histidine; and phenylalanine/leucine. Of the three  
232 sets containing histidine, only the leucine/histidine pair generates energy in the absence of the  
233 histidinol oxidoreductase activity. In addition, only the amount of ATP generated by the  
234 synthesis of leucine/histidine is significant: 2.33 mols of ATP (1.42 if the histidinol  
235 oxidoreductase is discarded) *per* mol produced of histidine/leucine versus 0.17 in the case of  
236 valine/histidine and 0.5 in the case of lysine/histidine. This suggests that only the set  
237 involving histidine and leucine can be considered energetic with reasonable certainty. The  
238 possibility of a certain amount of active transport, together with the high number of transport  
239 events required, suggests that the other histidine-containing pairs are probably not energetic

240 but, at least, cheap to produce.

241

242         Since the synthesis of phosphoenolpyruvate (essential precursor in aromatic amino  
243 acid production pathways) relies on either pyruvate or oxaloacetate, the four  
244 phenylalanine/leucine enEFMs can be classified into two groups: pyruvate-dependent or  
245 oxaloacetate-dependent. The reactions involved in each case are:

246



249

250         Because the *iJC86* model assumes that the recycling of AMP to ADP depends on the  
251 host, regarding energetics there are two significant differences between the two groups of  
252 phenylalanine/leucine enEFMs. Firstly, the usage of pyruvate involves more transport  
253 processes compared to oxaloacetate due to the recycling of AMP in the insect cytoplasm.  
254 Secondly, while the phosphoenolpyruvate synthesis via pyruvate generates one cytosolic H<sup>+</sup>,  
255 if oxaloacetate is used instead, one cytosolic H<sup>+</sup> is consumed. These differences explain why  
256 distinct enEFMs were identified, since the usage of oxaloacetate/pyruvate implies different  
257 reactions.

258

259         Another important property of the phenylalanine/leucine producing enEFMs is that  
260 they all depend on the presence of two non-essential orphan reactions. The absence of either  
261 D-glucose-6-phosphate isomerase or D-ribulose-5-phosphate-3-epimerase supposes the  
262 coupling of phenylalanine and tryptophan production (Figure 3). Because tryptophan is an  
263 expensive amino acid to produce in the network, this coupling could seriously restrict not

264 only the phenylalanine supply to the whitefly, but also the energetic effects of the  
265 endosymbiont. If we focus on the viability of the enEFMs studied above, oxalacetate-  
266 dependent ones produce 1.81 ATP *per* mol of amino acid while pyruvate-dependent ones  
267 produce 1.56 ATP *per* mol of amino acid. In this case the difference is slight, and both  
268 enEFMs can be considered energy-producing pathways.

269

270 For the characterization of the order two enEFMs to be complete, the contribution of the  
271 synthesis of each amino acid to the energy production must be identified. As can be seen in  
272 Table 3, the net production of NADPH is zero in each of these enEFMs. Because leucine,  
273 valine and lysine consume NADPH in their synthesis, the other amino acid must produce the  
274 same amount of reduced cofactor. In order to take advantage of this situation, a reaction that  
275 freely interchanges NADPH and NADP<sup>+</sup> was included in the model to obtain the energetic  
276 contribution of each amino acid in every energetic pair: if the synthesis of a particular amino  
277 acid in the pair produces ATP, new order one enEFMs must appear. The reason is that the  
278 inclusion of the NADP<sup>+</sup>-NADPH interchanging reaction buffers the NADPH consumed or  
279 generated during the synthesis of these amino acids and thus, it does not need to be obtained  
280 /redirected from another route. This analysis shows that leucine, valine and lysine are the ATP  
281 generators in the energetic pairs while histidine (or histidinol) and phenylalanine provide  
282 NADPH while consuming part of this ATP (Supplementary Table 3). As expected, leucine  
283 and lysine obtain ATP through the integration of NADH into the respiratory chain. However,  
284 no NADH is produced in the valine synthesis, with the ATP produced coming solely from the  
285 H<sup>+</sup> gap. This means that the production of valine consumes cytosolic H<sup>+</sup> that is excreted as  
286 part of other molecules (*e. g.* water), thereby increasing the electrochemical potential of H<sup>+</sup>  
287 and allowing ATP synthase to operate. This effect is present in other enEFMs, although this is

288 the only mode in which this effect is the unique source for ATP synthesis.

289

290 With respect to higher order enEFMs, the amino acids produced by each of these  
291 EFMs always include one of the amino acid pairs synthesized by second order enEFMs. This  
292 means that, by definition, there is no energetic amino acid sets with more than two  
293 components in any of the *iJC86* variants considered.

294

295 Although it is true that only pairs of amino acids were classified as energetic, it is  
296 possible that, when produced together or with other amino acids in the same enEFM, the flux  
297 distribution allows a higher production of energy than that expected from the order two  
298 enEFMs. These differences may be due to the utilization of a different pathway in the  
299 production of the energetic amino acids. However, when discounting the contribution of  $\beta$ -  
300 carotene and energetic amino acids synthesis, no such effects were observed. Finally, the case  
301 of energetically self-sufficient EFMs which produce amino acids was considered. However,  
302 no EFM matching this criterion was found.

303

### 304 **The role of $\beta$ -carotene synthesis in the metabolic capabilities of *Portiera***

305 One remarkable feature of *Portiera*'s metabolism involves the ATP production  
306 associated with  $\beta$ -carotene synthesis. It is worth to note that the turnover of this molecule may  
307 not be high enough to support *Portiera*'s energetic needs. If this was the case, the remaining  
308 ATP requirements should be satisfied by a non-negative combination of non-zero order  
309 enEFMs. This implies that, in order to growth, the endosymbiont may overproduce certain  
310 amino acids. To study this phenomenon the maximum biomass produced and the magnitude  
311 and nature of the overproductions were determined after constraining the flux through  $\beta$ -

312 carotene synthesis to different values (from zero to unbounded). Because the majority of the  
313 amino acid production may be destined to the insect, a reaction representing the whitefly  
314 biomass was included in the model and several ratios of endosymbiont biomass to insect  
315 biomass were evaluated (see Methods). Since no specific information on the amino acid  
316 composition and ATP requirements of either the whitefly or *Portiera* was found in the  
317 literature, the simulations were performed using an ensemble of randomized biomass  
318 equations derived from those corresponding to *A. pisum* and *E. coli*, respectively (see  
319 Methods). It is important to note that the ATP requirement for the whitefly biomass equation  
320 in *iJC86* is expected to be zero. The reason for this expectation is that the cost of assembling  
321 the proteins needed for the insect is assumed by the insect itself and thus, is not included in  
322 the model. Thus, the ATP cost of the biomass equations of the whitefly was set to be zero (see  
323 Methods). The most relevant findings obtained through this analysis are displayed in Figure 4.  
324

325         Because the differences in the amino acid compositions of the two biomasses are less  
326 marked than the corresponding to ATP consumption, it can be assumed that an increase in the  
327 endosymbiont to insect biomass ratio is equivalent to an increase in the ATP requirements for  
328 the whole system (whitefly plus *Portiera*) to grow. Thus, attending to the results presented in  
329 the previous section, an increment in the overproduction of amino acids is expected. Results  
330 from constraining the flux through  $\beta$ -carotene synthesis demonstrate this point: as the ratio of  
331 endosymbiont biomass to insect biomass is increased, the total biomass produced (insect plus  
332 endosymbiont) quickly decreases at the same rate as the flux of overproduced amino acids  
333 increases (Figure 4).

334

335         The effect on biomass production seems to be independent of the constraint in  $\beta$ -

336 carotene synthesis but not for the amino acid overflows (Figure 4). If the  $\beta$ -carotene  
337 production accounts for at least around 60% of the total carbon source flux, no amino acid  
338 overflow is observed irrespective of the value of the symbiont-to-insect biomass ratio. This  
339 suggests that, assuming the most relaxed case (symbiont-to-insect biomass ratio = 1:100 in the  
340 model with all the orphan reactions of Table 1 included), the number of  $\beta$ -carotene molecules  
341 produced *per* amino acid destined to biomass is at least 2. Because a minimum of 90% of the  
342 biomass maximum was set in these analyses, we asked at what fraction of the biomass  
343 maximum (if this maximum exists) will there be no  $\beta$ -carotene production and no amino acid  
344 overflow. Restricting the  $\beta$ -carotene and amino acid exchange fluxes to zero impedes the  
345 growth of the system, whatever the symbiont-to-insect biomass ratio. Even if this condition is  
346 relaxed (by allowing a maximum flux through these reactions of 1% of the total carbon source  
347 flux allowed to enter the symbiont), less than 10% of the maximum biomass is produced in  
348 the corresponding models without these constraints. Taking these results as a whole, for  
349 *Portiera* (no matter which orphan reactions are included in the model, see Table 1) to work in  
350 near-optimal (>90% of the maximum, as above assessed) biomass-producing conditions (either  
351 for itself or for the insect) it must either overproduce amino acids or  $\beta$ -carotene.

352

353         If we consider the nature of the overproduced amino acids (Figure 4), it is not  
354 surprising that leucine and histidine/histidinol are the ones which are overproduced. As  
355 mentioned above, the leucine-histidine/histidinol and phenylalanine-leucine pairs are  
356 associated with the most effective second order enEFMs, with respect to the amount of ATP  
357 synthesized. Because leucine participates in all the pairs named, it is overproduced in higher  
358 amounts than histidine/histidinol. Phenylalanine is not overproduced essentially because it is  
359 required in higher amounts in the biomass equations compared to histidine, and because the

360 leucine-histidine pair produces approximately 0.5 ATP molecules *per* amino acid, which is  
361 more than the best phenylalanine-leucine-producing enEFM.

362

### 363 **Discussion**

364

365 The results of the stoichiometric analysis of the *iJC86* model with regard to the amino  
366 acid metabolism are consistent with all previous studies on metabolic complementation  
367 between *Portiera* and its insect host. In addition, these complementations resemble those  
368 reported in *Buchnera aphidicola*, the endosymbiont of the aphid *Acyrtosiphon pisum*(17,  
369 18). Most of these studies are based either on qualitative genome analysis(11, 12, 14) or on  
370 experimental approaches (e.g. transcriptome analysis(13, 15)). A curated model, such as the  
371 here presented *iJC86* , offers additional opportunities for investigating the structural  
372 properties of the metabolic network with a systems biology approach, such as the EFM  
373 analysis. According to the *iJC86* model, the energetics of *Portiera* relies (with the exception  
374 of the spontaneous proton-motive force generated in the synthesis of valine) entirely on its  
375 respiratory chain: all the ATP produced comes from either the oxidation of the ubiquinol  
376 produced in the formation of the double-bonds of the  $\beta$ -carotene or the oxidation of the  
377 NADH generated during the synthesis of certain amino acid pairs (Figure 2). These pairs are  
378 established because the NADPH balance must be maintained. In particular, they involve a  
379 NADPH-consuming/energy-producing amino acid (leucine, valine or lysine) and a NADPH-  
380 producing/energy-consuming one (phenylalanine, histidine/histidinol). The remaining amino  
381 acids (arginine, threonine, tryptophan and isoleucine) are all energy dependant. The amount of  
382 energy produced in association with the synthesis of these amino acids ranges from 0.17 to  
383 2.33 moles of ATP *per* mol of amino acid produced (Table 3). However, these results only



384 hold if all the transport processes in *Portiera* are assumed to be passive. Although this  
385 assumption is reasonable considering the high concentration of sugars and non-essential  
386 amino acids in the insect diet(19), it may not be wholly valid. Minor deviations from the all-  
387 passive transport assumption has important consequences when considering the energetics of  
388 *Portiera*. Essentially, the ATP production associated with the valine/histidine and  
389 lysine/histidine pairs would be abolished, leaving  $\beta$ -carotene and leucine production as the  
390 energetic motor of the symbiont. This situation highlights the importance of the knowledge  
391 gap regarding the transport processes in endosymbionts when analyzing their metabolic  
392 networks: the behavior of the network can vary dramatically under slightly different  
393 scenarios. Nevertheless, the passive transport assumption allows all possible functionalities of  
394 the network to be considered, and robust behaviors can be identified, such as the case of  $\beta$ -  
395 carotene or the leucine pairs discussed previously.

396

397 Two remarkable features were revealed through the modelling of *Portiera*'s energetic  
398 metabolism. The first one comprises the production of ATP associated with valine synthesis  
399 (Supplementary Table 3). Because no substrate-level phosphorylation exists in the network,  
400 an energy production independent of the respiratory chain was unexpected, and raises the  
401 question of how the endosymbiont can generate the electrochemical proton gradient needed  
402 for the ATP synthase to operate. According to the *iJC86* model predictions, the proton motive  
403 force needed is obtained through the exportation of cytosolic protons by including them in the  
404 structure of other molecules. Symmetrically, this contribution to the generation of proton  
405 motive force, defined here as a proton gap, can also be detrimental to energy production if  
406 protons are generated instead of consumed. The effects of the proton gap on the symbiont  
407 energetics are widespread and significant in the majority of cases (SupplementaryTable 3).

408 Because this effect is only predicted using stoichiometric analysis, empirical tests should also  
409 be used to assess its role in the system.

410

411 A second remarkable feature of *Portiera*'s metabolism involves the  $\beta$ -carotene  
412 synthesis. Carotenoids and their derivatives have important functions in insects, such as  
413 coloration, vision, diapause, photoperiodism, mate choice or oxidative stress(20). The  
414 stoichiometric analysis of the *iJC86* model reveals an additional possible function related to  
415 energetics and, ultimately, to the control of amino acid biosynthesis. Leucine, lysine, valine  
416 and, to a lesser extent, phenylalanine and tyrosine (obtained through phenylalanine oxidation),  
417 span a notable percentage of the proteome not only in insects(21) but also in other  
418 organisms(22). In contrast, histidine is only required in small quantities(21, 22). If no  $\beta$ -  
419 carotene-associated ATP production exists, *Portiera* will produce an excess of certain amino  
420 acids with a significant overproduction of leucine and histidine (Figure 4). However, if  $\beta$ -  
421 carotene-associated ATP production is allowed, this restriction can be avoided. Nevertheless,  
422 the minimum amount of  $\beta$ -carotene synthesis needed for neglecting amino acid production is  
423 about two times the production of amino acids, if all of them are destined to the whitefly, and  
424 much more if we also consider *Portiera*'s growth. Thus, for the insect-endosymbiont system  
425 to growth with a significant yield (>10% of its maximum), either leucine and histidine or  $\beta$ -  
426 carotene must be substantially overproduced. This performance suggests two non-exclusive  
427 possible scenarios: the overproduced substances have a particular physiological or ecological  
428 (*e.g.* through excretion in honeydew) function for the whitefly, or they have no significant  
429 fitness effect in the system. However, a third scenario can be conceived taking into  
430 consideration recent evidence(23) which suggests that  $\beta$ -carotene could be involved in light-  
431 induced reduction of NAD<sup>+</sup> in insects. Thus, if light can induce a cyclic electron transport in

432 which the NADH oxidation through NADH-dehydrogenase takes part, ATP can be  
433 synthesized without the concomitant production of amino acids or  $\beta$ -carotene. Assuming  
434 this as true, its energetic role in *Portiera* is independent of the amount of  $\beta$ -carotene  
435 synthesized, and thus overproduction of any kind is unexpected.

436

437 It is worth to emphasise that the properties inferred from *iJC86* model of *Portiera*'s  
438 panmetabolism can be extrapolated to similar networks with few additional considerations.  
439 Lets consider two examples. Attending to comparative genomics(14), the only *Portiera* strain  
440 which deviate significantly from the others is *Candidatus Portiera aleyrodidarum* BT-QVLC,  
441 hosted in *B. tabaci*. Specifically, this strain lacks genes involved in lysine (*dapB*, *dapF* and  
442 *lysA*) and arginine (*argG* and *argH*) synthesis(14, 15). The inspection of the reactions  
443 associated to *dapB*, *dapF* and *lysA* shows that they contribute with 0.25 ATP *per* amino acid  
444 (by increasing the proton gap by one *per* amino acid) to the net production of 0.5 ATP *per*  
445 amino acid associated to the enEFM's in which lysine is produced (Table 2). Because arginine  
446 synthesis is not associated by any means to ATP or NADPH production, it can be concluded  
447 that the energy metabolism of *Candidatus Portiera aleyrodidarum* BT-QVLC is essentially the  
448 same than the one inferred from *iJC86* model of *Portiera*'s panmetabolism. Let consider now  
449 the effects on the network of allowing the importation of phosphoenolpyruvate (PEP) in  
450 *Portiera*'s energy metabolism. The only destination of this metabolite in the network is the  
451 production of phenylalanine. Attending to Supplementary Table 3, the cost of synthesizing  
452 this amino acid depends, precisely, on the precursor employed in the production of PEP.  
453 Thus, by discounting the contribution of PEP synthesis to those enEFM associated to  
454 phenylalanine production, the effects of the free importation of PEP on the energy metabolism  
455 of *Portiera* can be determined. In particular, a new order two enEFM synthesizing

456 phenylalanine/leucine will appear with an associated net production of  $\sim 2.06$  ATP *per* amino  
457 acid, in contrast to the  $\sim 1.86$  and  $\sim 1.56$  ATP obtained if PEP is produced from oxaloacetate  
458 and pyruvate, respectively. Again, no substantial changes appear if a free incorporation of  
459 PEP is considered, the main reason being that the more efficient ATP production in the  
460 network is still associated to the synthesis of  $\beta$ -carotene ( $2.5$  ATP *per*  $\beta$ -carotene) and the  
461 pair leucine/histidine ( $\sim 2.33$  ATP *per* amino acid).

462

463 In conclusion, *Portiera* shows the capability of simultaneously providing the whitefly  
464 with nine essential amino acids while being capable of synthesizing its own ATP. The ways  
465 nature has allowed this to be possible involve the efficient configuration of biosynthesis  
466 pathways that reduces the catabolic reactions needed to a minimum. This configuration is  
467 especially notable when  $\beta$ -carotene synthesis is considered: just a few reactions allow a coarse  
468 control of amino acid production while serving as fuel for this particular ATP-synthesis  
469 machinery. Because *Portiera* is just one of a number of reduced genome endosymbionts, it  
470 serves as a milestone in the exploration of the energetics of these organisms.

471

## 472 **Methods**

### 473 **Elementary Flux Modes Analysis**

474 Computation of the elementary modes (EFMs) was performed on a modified version  
475 of *iJC86*, where an ATP consumption reaction (referred to as *energy*) was incorporated as a  
476 label for the identification of enEFMs. EFMs in which *energy* is greater than zero are the  
477 enEFMs of the model (see *definition 1* in results). The set of EFMs was calculated using the  
478 EFMtool(24).

479

480 **Determination of the impact of  $\beta$ -carotene synthesis on the metabolic performance of**  
481 ***iJC86*.**

482 In order to perform this analysis the model was reconfigured to represent the *Portiera*-  
483 whitefly interaction in a more realistic way. First, a simplified biomass equation representing  
484 the amino acid demands required for the insect's growth was added to the system, using the  
485 amino acid content of *A. pisum* as a reference(21). In particular, each amino acid produced by  
486 *Portiera* was added as a reactant with a stoichiometric coefficient equal to its content in *A.*  
487 *pisum* (with the exception of phenylalanine, whose coefficient also includes the content of  
488 tyrosine because the last one is a necessary precursor of the first one). Once the stoichiometric  
489 coefficients were set, they were normalized for their summation to be one.

490

491 Due to the fact that the relation of both biomass productions is unknown, several  
492 symbiont-to-insect biomass ratios were tested. For each of these ratios, the maximum biomass  
493 production of the system (insect+symbiont) was calculated through flux balance analysis(25),  
494 after constraining the  $\beta$ -carotene exportation flux to several values  $C \in [0, 100]$ . Then, for  
495 each  $C$ , the overproduction of every amino acid was evaluated by considering the minimum  
496 value computed using flux variability analysis(24) (biomass flux >90% of its maximum).

497

498 To fulfil the previous calculations, the model's reactions were considered as  
499 unbounded by setting their upper bounds to  $10^6$  arbitrary flux units (AFUs) and their lower  
500 bounds to 0 or  $-10^6$  AFUs for reversible reactions. Moreover, a constraint to limit the  
501 maximum carbon sources (CS) importation was incorporated:

502

503 
$$\sum_{i \in CS} v_i \leq K \quad (2)$$

504

505 where  $CS$  includes glucose, pyruvate, oxaloacetate,  $\alpha$ -ketoglutarate, ornithine, aspartate, and  
506 geranylgeranyl diphosphate;  $v_i$  is the flux through the corresponding transportation reaction  
507 and  $K$  is the value of the constraint. The value of  $K$  was fixed to 100 AFUs in order to make it  
508 the only active constraint in the model.

509

510 Since no specific information on the amino acid composition of either the whitefly or  
511 *Portiera* was found in the literature, the experiments were performed using an ensemble of  
512 100 randomized variants of the biomass equations to make the results obtained more robust.  
513 The randomization was conducted in the following way: for each amino acid the  
514 stoichiometric coefficient was drawn from a uniform distribution in the interval  $(0.75 x_0,$   
515  $1.25x_0)$  where  $x_0$  corresponds to the reference value. These values were normalized  
516 afterwards as mentioned above. The ATP consumption for the insect and symbiont production  
517 was then modified. For the insect, the ATP cost was set to zero. On the other hand, the ATP  
518 cost associated to the symbiont biomass equation was extracted from a uniform distribution in  
519 the interval  $[30,70]$ .

520

## 521 **Computational Tools**

522 Constraint-based analysis was performed using the python-based toolbox  
523 COBRApy(26). LP and MILP problems were solved using the Gurobi Solver(27) accessed  
524 through COBRApy. The computation of connected components for the detection of the set of  
525 unconnected modules was performed using the Python NetworkX library(28). The scripts  
526 developed for this paper were programmed in Python language(29), and can be requested  
527 from the authors. Graphs were drawn using the yEd Graph Editor(30). All the computations

528 were performed on a workstation using an Intel® Xeon® CPU X5660 2.80GHz processor,  
529 with 32GiB, running under Ubuntu 14.04.2 Linux OS.

## 530 **References**

- 531 1. Baumann, P. 2005. Biology bacteriocyte-associated endosymbionts of plant sap-  
532 sucking insects. *Annu. Rev. Microbiol.* 59: 155–89.
- 533 2. Moya, A., J. Peretó, R. Gil, and A. Latorre. 2008. Learning how to live together:  
534 genomic insights into prokaryote-animal symbioses. *Nat. Rev. Genet.* 9: 218–29.
- 535 3. McCutcheon, J.P., and N.A. Moran. 2012. Extreme genome reduction in symbiotic  
536 bacteria. *Nat. Rev. Microbiol.* 10: 13–26.
- 537 4. Cottret, L., P.V. Milreu, V. Acuña, A. Marchetti-Spaccamela, L. Stougie, H. Charles,  
538 and M.-F. Sagot. 2010. Graph-based analysis of the metabolic exchanges between two  
539 co-resident intracellular symbionts, *Baumannia cicadellincola* and *Sulcia muelleri*,  
540 with their insect host, *Homalodisca coagulata*. *PLoS Comput. Biol.* 6: e1000904.
- 541 5. González-Domenech, C.M., E. Belda, R. Patiño-Navarrete, A. Moya, J. Peretó, and A.  
542 Latorre. 2012. Metabolic stasis in an ancient symbiosis: genome-scale metabolic  
543 networks from two *Blattabacterium cuenoti* strains, primary endosymbionts of  
544 cockroaches. *BMC Microbiol.* 12 Suppl 1: S5.
- 545 6. Ponce-de-León, M., F. Montero, and J. Peretó. 2013. Solving gap metabolites and  
546 blocked reactions in genome-scale models: application to the metabolic network of  
547 *Blattabacterium cuenoti*. *BMC Syst. Biol.* 7: 114.
- 548 7. Thomas, G.H., J. Zucker, S.J. Macdonald, A. Sorokin, I. Goryanin, and A.E. Douglas.  
549 2009. A fragile metabolic network adapted for cooperation in the symbiotic bacterium  
550 *Buchnera aphidicola*. *BMC Syst. Biol.* 3: 24.
- 551 8. Belda, E., F.J. Silva, J. Peretó, and A. Moya. 2012. Metabolic networks of *Sodalis*  
552 *glossinidius*: a systems biology approach to reductive evolution. *PLoS One.* 7: e30652.
- 553 9. Thao, M.L., and P. Baumann. 2004. Evolutionary relationships of primary prokaryotic  
554 endosymbionts of whiteflies and their hosts. *Appl. Environ. Microbiol.* 70: 3401–6.
- 555 10. Moran, N.A., and G.M. Bennett. 2014. The tiniest tiny genomes. *Annu. Rev.*  
556 *Microbiol.* 68: 195–215.
- 557 11. Santos-Garcia, D., P.-A. Farnier, F. Beitia, E. Zchori-Fein, F. Vavre, L. Mouton, A.  
558 Moya, A. Latorre, and F.J. Silva. 2012. Complete genome sequence of “*Candidatus*  
559 *Portiera aleyrodidarum*” BT-QVLC, an obligate symbiont that supplies amino acids  
560 and carotenoids to *Bemisia tabaci*. *J. Bacteriol.* 194: 6654–5.
- 561 12. Rao, Q., P.-A. Rollat-Farnier, D.-T. Zhu, D. Santos-Garcia, F.J. Silva, A. Moya, A.

- 562 Latorre, C.C. Klein, F. Vavre, M.-F. Sagot, S.-S. Liu, L. Mouton, and X.-W. Wang.  
563 2015. Genome reduction and potential metabolic complementation of the dual  
564 endosymbionts in the whitefly *Bemisia tabaci*. *BMC Genomics*. 16: 226.
- 565 13. Upadhyay, S.K., S. Sharma, H. Singh, S. Dixit, J. Kumar, P.C. Verma, and K.  
566 Chandrashekar. 2015. Whitefly Genome Expression Reveals Host-Symbiont  
567 Interaction in Amino Acid Biosynthesis. *PLoS One*. 10: e0126751.
- 568 14. Santos-Garcia, D., C. Vargas-Chavez, A. Moya, A. Latorre, and F.J. Silva. 2015.  
569 Genome evolution in the primary endosymbiont of whiteflies sheds light on their  
570 divergence. *Genome Biol. Evol.* 7: 873–88.
- 571 15. Luan, J.-B., W. Chen, D.K. Hasegawa, A.M. Simmons, W.M. Wintermantel, K.-S.  
572 Ling, Z. Fei, S.-S. Liu, and A.E. Douglas. 2015. Metabolic Coevolution in the Bacterial  
573 Symbiosis of Whiteflies and Related Plant Sap-Feeding Insects. *Genome Biol. Evol.* 7:  
574 2635–47.
- 575 16. Overbeek, R., T. Begley, R.M. Butler, J. V Choudhuri, H.-Y. Chuang, M. Cohoon, V.  
576 de Crécy-Lagard, N. Diaz, T. Disz, R. Edwards, M. Fonstein, E.D. Frank, S. Gerdes,  
577 E.M. Glass, A. Goesmann, A. Hanson, D. Iwata-Reuyl, R. Jensen, N. Jamshidi, L.  
578 Krause, M. Kubal, N. Larsen, B. Linke, A.C. McHardy, F. Meyer, H. Neuweger, G.  
579 Olsen, R. Olson, A. Osterman, V. Portnoy, G.D. Pusch, D.A. Rodionov, C. Rückert, J.  
580 Steiner, R. Stevens, I. Thiele, O. Vassieva, Y. Ye, O. Zagnitko, and V. Vonstein. 2005.  
581 The subsystems approach to genome annotation and its use in the project to annotate  
582 1000 genomes. *Nucleic Acids Res.* 33: 5691–702.
- 583 17. Hansen, A.K., and N.A. Moran. 2011. Aphid genome expression reveals host-symbiont  
584 cooperation in the production of amino acids. *Proc. Natl. Acad. Sci. U. S. A.* 108:  
585 2849–54.
- 586 18. Macdonald, S.J., G.G. Lin, C.W. Russell, G.H. Thomas, and A.E. Douglas. 2012. The  
587 central role of the host cell in symbiotic nitrogen metabolism. *Proc. Biol. Sci.* 279:  
588 2965–73.
- 589 19. Dinant, S., J.-L. Bonnemain, C. Girousse, and J. Kehr. Phloem sap intricacy and  
590 interplay with aphid feeding. *C. R. Biol.* 333: 504–15.
- 591 20. Cazzonelli, C.I. 2011. Goldacre Review: Carotenoids in nature: insights from plants  
592 and beyond. *Funct. Plant Biol.* 38: 833.
- 593 21. Russell, C.W., A. Poliakov, M. Haribal, G. Jander, K.J. van Wijk, and A.E. Douglas.  
594 2014. Matching the supply of bacterial nutrients to the nutritional demand of the animal  
595 host. *Proc. Biol. Sci.* 281: 20141163.
- 596 22. Sorimachi, K. 2009. Evolution from Primitive Life to Homo sapiens Based on Visible  
597 Genome Structures: The Amino Acid World. *Nat. Sci.* 01: 107–119.



- 598 23. Valmalette, J.C., A. Dombrovsky, P. Brat, C. Mertz, M. Capovilla, and A. Robichon.  
599 2012. Light- induced electron transfer and ATP synthesis in a carotene synthesizing  
600 insect. *Sci. Rep.* 2: 579.
- 601 24. Terzer, M., and J. Stelling. 2008. Large-scale computation of elementary flux modes  
602 with bit pattern trees. *Bioinformatics.* 24: 2229–35.
- 603 25. Orth, J.D., I. Thiele, and B.Ø. Palsson. 2010. What is flux balance analysis? *Nat.*  
604 *Biotechnol.* 28: 245–8.
- 605 26. Ebrahim, A., J.A. Lerman, B.O. Palsson, and D.R. Hyduke. 2013. COBRApy:  
606 COstraints-Based Reconstruction and Analysis for Python. *BMC Syst. Biol.* 7: 74.
- 607 27. Gurobi Optimization, I. 2012. Houston, Texas: Gurobi Optimization, Inc. .
- 608 28. Hagberg, A.A., D.A. Schult, and P.J. Swart. 2008. Exploring network structure,  
609 dynamics, and function using {NetworkX}. In: *Proceedings of the 7th Python in  
610 Science Conference (SciPy2008)*. Pasadena, CA USA: . pp. 11–15.
- 611 29. Jones, E., T. Oliphant, P. Peterson, and others. *SciPy: Open source scientific tools for  
612 Python*. PythonLabs, Virginia, USA. .

613

614

615

616

617

618

619

620

621

622

623

624

625

626 **Acknowledgements**

627 We would like to thank the Obra Social Programme of *La Caixa* Savings Bank for the  
628 doctoral fellowship granted to JCE. Financial support from the Spanish Government (grant  
629 reference: BFU2012-39816-C02-01 and BFU2012-39816-C02-02, co-financed by FEDER  
630 funds and the Ministry of the Economy and Competitiveness) and the Regional Government  
631 of Valencia (grant reference: PROMETEOII/2014/065) is also gratefully acknowledged.

632

633 **Contributions**

634 F.J.S. and D.S.G. provided functionally annotated genomic data prior to publication; J.C.E.  
635 and M.P.L. performed the experiments; J.C.E, M.P.L, F.M and J.P. analyzed the data; J.C.E.  
636 wrote the manuscript with inputs from M.P.L, F.M., D.S.G., F.J.S. and J.P. All authors read  
637 and approved the final manuscript.

638 **Competing financial interests**

639 The authors declare no competing financial interests.

640

641 **Figure Captions**

642 **Figure 1: Metabolic complementations suggested by the *iJC86* model.** Exchange of  
643 glutamate and  $\alpha$ -ketoglutarate: the endosymbiont uses glutamate for transamination reactions  
644 and the produced  $\alpha$ -ketoglutarate is exported to the bacteriocyte. Exchange of AICAR and  
645 purine bases (and its derivatives): the endosymbiont generates AICAR as a subproduct of  
646 histidine biosynthesis and exports it to the bacteriocyte, where it is recycled into purine bases  
647 for the use of both the endosymbiont and its host.  $\beta$ -carotene production: whitefly provides  
648 geranylgeranyl diphosphate for the synthesis of  $\beta$ -carotene. This process requires the  
649 reduction of quinone to quinol, which is then oxidized by the respiratory chain. Exportation of  
650 succinate and fumarate: the synthesis of lysine and arginine involves the production of  
651 succinate and fumarate, respectively, compounds that must be consumed by the host. gg-PPi,  
652 geranylgeranyl diphosphate; Isocit, isocitrate; Cit, citrate; Oxaloac, oxaloacetate; Mal,  
653 malate; Fum, fumarate; Succ, succinate; Succ-Coa, succinyl-CoA;  $\alpha$ -ketoglu,  $\alpha$ -ketoglutarate;  
654 AICAR, 5-amino-1-ribofuranosyl-imidazole-4-carboxamide; PRPP, phosphoribosyl  
655 pyrophosphate; Orn, ornithine; GS, glutamine synthetase; GOGAT, glutamine: $\alpha$ -ketoglutarate  
656 aminotransferase.

657

658 **Figure 2: Representation of the energetics of *Portiera* according to the *iJC86* model.**

659 The only zero order enEFM of the *iJC86* model involves the synthesis of  $\beta$ -carotene. In this  
660 pathway the geranylgeranyl diphosphate is oxidized by quinones, which are then incorporated  
661 into the respiratory chain in the form of quinol, generating ATP through oxidative  
662 phosphorylation. Every non-zero order enEFM is associated with the production of at least  
663 two amino acids, one associated with the production of NADPH (phenylalanine or  
664 histidine/histidinol) and the other with its consumption (leucine, valine or lysine). The number

665 of ATP molecules generated (red) /consumed (blue) *per* molecule of amino acid or amount of  
666  $\beta$ -carotene produced is represented by the thickness of the arrows. Dotted arrows represent  
667 pathways in which ATP synthesis is associated only with the gradient generated through the  
668 consumption of intracellular protons. PRPP, phosphoribosyl pyrophosphate.

669

670 **Figure 3: Graph representing the coupling between phenylalanine and tryptophan**  
671 **biosynthesis in *iJC86* model of *P. aleyrodidarum* metabolism if D-ribulose-5-phosphate-**  
672 **3-epimerase and D-glucose-6-phosphate isomerase are not included as orphan.**

673 Metabolites are represented with their abridged name and reactions are represented as  
674 softened rectangles containing the corresponding EC number. ru5p-D\_c, ribulose-5-  
675 phosphate; g3p\_c, glyceraldehyde 3-phosphate; s7p\_c, sedoheptulose-7-phosphate; f6p\_c,  
676 fructose-6-phosphate; e4p\_c, erythrose-4-phosphate; xu5p-D\_c, xylulose-5-phosphate.

677

678 **Figure 4: Impact of  $\beta$ -carotene synthesis on the metabolic performance of the *iJC86* model**

679 **of *Portiera's* metabolism.** Representation of the effect of  $\beta$ -carotene synthesis in maximum  
680 insect biomass production (green) and amino acid overflows (histidine, blue; leucine,  
681 magenta; histidine + leucine, black). Because part of the insect's biomass corresponds to  
682 *Portiera*, several symbiont-to-insect biomass ratios were tested (panels *a*, *b*, *c* and *d*). For  
683 each ratio, the 90% of maximum biomass production, in addition to the overflow of each  
684 produced amino acid were calculated under different constraints on the  $\beta$ -carotene synthesis  
685 (*max crt*): from 0% to 100% of the total carbon sources flux. Only leucine and histidine were  
686 detected to be overproduced. Due to the lack of specific information regarding the biomass  
687 equation of either *Portiera* or the whitefly, the simulation described above was carried on an  
688 ensemble of 100 randomized variants of these equations (see *Methods*). The results plotted

689 here accounts for the mean of all simulations, error bars representing the corresponding  
690 standard deviation. *AFU*: arbitrary flux units.

## 691 TABLES

692 **Table 1: Orphan reactions of the *iJC86* model of *Portiera's* metabolism.** Reactions in bold  
693 could be substituted by a proper complementation with the host. Reactions labelled with a (\*) are  
694 not essential for biomass production by *iJC86*. At least one of the reactions labelled with a (▲)  
695 must be active for biomass production by *iJC86*. BCA, branched-chain amino acid.

696

REACTION	GENE	PATHWAY
<b>histidinol dehydrogenase</b>	<i>hisD</i>	<b>histidine biosynthesis</b>
<b>histidinal dehydrogenase</b>	<i>hisD</i>	<b>histidine biosynthesis</b>
phosphoenolpyruvate synthetase ▲	<i>pps</i>	chorismate biosynthesis
phosphoenolpyruvate carboxykinase ▲	<i>pck</i>	chorismate biosynthesis
transaldolase	<i>talB</i>	pentose phosphate pathway
ribose-5P-isomerase	<i>rpiA/B</i>	pentose phosphate pathway
phosphogluconolactonase	<i>spontaneous/pgl</i>	pentose phosphate pathway
ribulose-5P-3-epimerase *	<i>rpe</i>	pentose phosphate pathway
glucose-6P-isomerase *	<i>pgi</i>	pentose phosphate pathway
<b>leucine transaminase</b>	<i>ilvE</i>	<b>BCA biosynthesis</b>
<b>isoleucine transaminase</b>	<i>ilvE</i>	<b>BCA biosynthesis</b>
<b>valine transaminase</b>	<i>ilvE</i>	<b>BCA biosynthesis</b>
<b>carbonic anhydrase</b>	<i>yadF/cynT/spontaneous</i>	<b>arginine biosynthesis</b>

698

699

700

701 **Table 2: Characteristics of the *iJC86* model of *Portiera's* metabolism.** The first block displays  
702 the inputs and outputs needed for  $\beta$ -carotene and each amino acid to be produced. All the  
703 compounds in this block are essential for the whitefly. The second block contains those  
704 compounds (excluding ions), which are essential for the network to be functional and produce  
705 biomass. TPP, thiamine pyrophosphate; AICAR, 5-amino-1-ribofuranosyl-imidazole-4-  
706 carboxamide.  
707

	INPUTS	OUTPUTS
<i>leucine</i>	D-glucose, pyruvate/oxaloacetate, ADP	$\alpha$ -ketoglutarate, AMP
<i>valine</i>	D-glucose, pyruvate/oxaloacetate, ADP	$\alpha$ -ketoglutarate, AMP
<i>isoleucine</i>	D-glucose, pyruvate/oxaloacetate, aspartate, ADP	$\alpha$ -ketoglutarate, AMP
<i>tryptophan</i>	D-glucose, pyruvate/oxaloacetate, ADP, serine	$\alpha$ -ketoglutarate, AMP
<i>phenylalanine</i>	D-glucose, pyruvate/oxaloacetate, ADP	$\alpha$ -ketoglutarate, AMP
<i>threonine</i>	D-glucose, aspartate, ADP	$\alpha$ -ketoglutarate, AMP
<i>lysine</i>	D-glucose, pyruvate/oxaloacetate, aspartate, ADP	succinate, $\alpha$ -ketoglutarate, AMP
<i>arginine</i>	aspartate, glutamine, ornithine, ADP	fumarate, AMP
<i>histidine</i>	D-glucose, glutamine, ADP	AICAR, $\alpha$ -ketoglutarate, AMP
<i>B-carotene</i>	geranylgeranyl diphosphate	---
<b>BIOMASS</b>	D-glucose, pyruvate/oxaloacetate	fumarate, succinate, $\alpha$ -ketoglutarate
	alanine, proline, glycine, serine, glutamine, glutamate, asparagine, aspartate, cysteine, methionine, tyrosine, ornithine	---
	ubiquinone-8/menaquinone-8, lipoamide, coenzyme A, NAD <sup>+</sup> , NADP <sup>+</sup> , TPP	---
	nitrogenous bases and derivatives, lipids	AICAR, AMP

709

710 **Table 3: Properties of the EFMs related to the energetic productions of the *iJC86* model of**

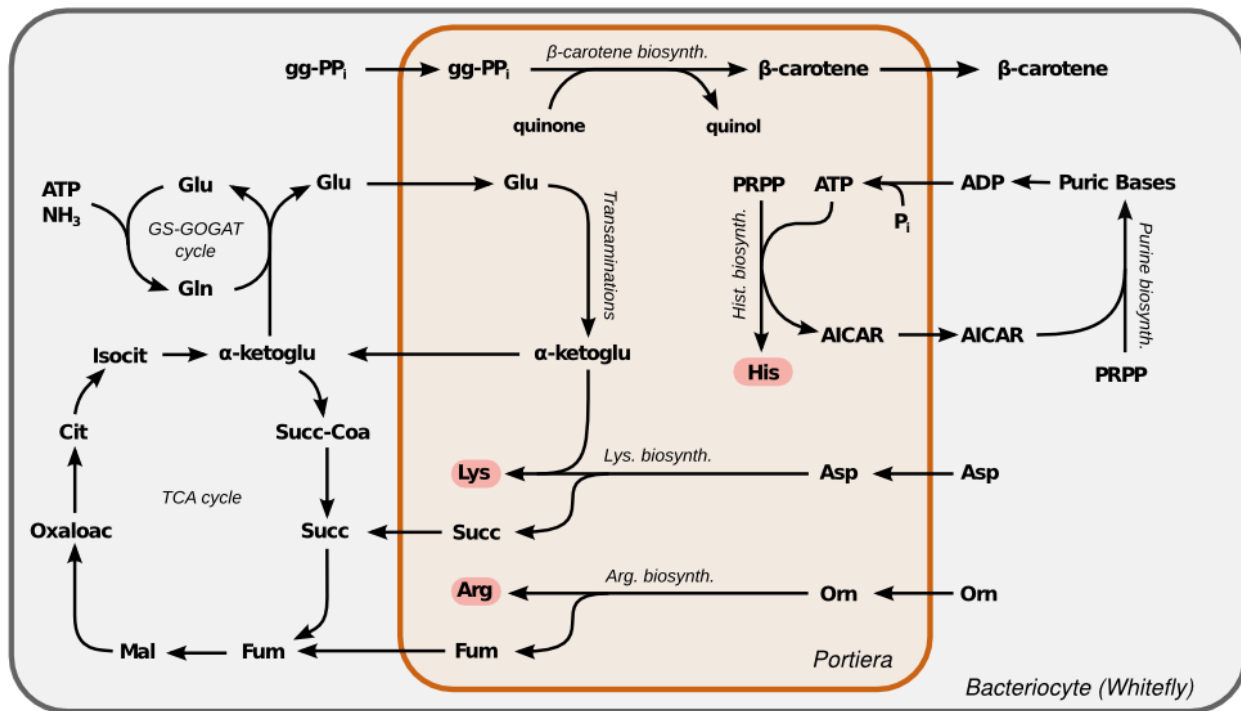
711 **Portiera.** For each order (first column), the corresponding amino acid sets ( $\beta$ -carotene for order  
712 zero) are displayed in the second column, while the associated properties are listed in the next  
713 ones. The properties listed are: net NADPH production ( $\Delta$ NADPH); net NADH production  
714 ( $\Delta$ NADH); ATP consumed ( $ATP_{cons}$ ); proton gap ( $H^+$ gap); net ATP produced ( $\Delta$ ATP); ATP  
715 produced due to the proton gap ( $S_{H^+}$ ); and number of transported molecules (trans). Data are  
716 based on the production of 1 arbitrary flux unit of amino acid. The requests for each enEFM  
717 regarding the presence (+) or absence (-) of a variant-specific reaction are indicated as follows:  
718 requirement of D-ribulose-5-phosphate epimerase (p1) or D-glucose-6-phosphate isomerase (p2),  
719 both defining the *iJC86 p*- model; oxaloacetate-dependent phosphoenolpyruvate production (o);  
720 requirement of histidinol oxidoreductase (h). The number of enEFMs associated with each  
721 energetic amino acid set and each particular property are displayed in the last column. For every  
722 second order EFM the contribution of each amino acid is displayed (see Ratio column). The  
723 contribution of  $\beta$ -carotene biosynthesis was discounted in every EFM, which relies on it. Histsd,  
724 histidinol.

725

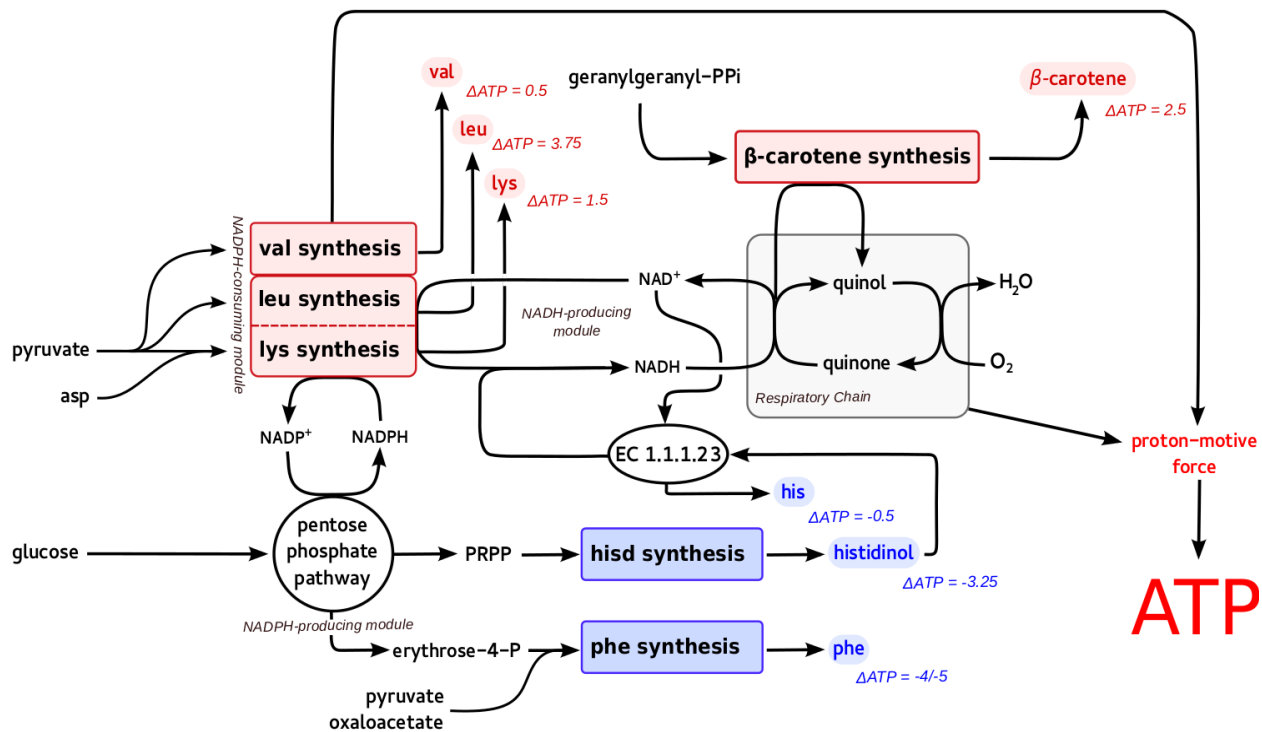
order	products	$\Delta$ NADPH	$\Delta$ NADH	$ATP_{cons}$	$H^+$ gap	$\Delta$ ATP	$S_{H^+}$	trans.	p1	p2	o	h	ratio	enEFM
<i>zero</i>	$\beta$ -carotene	0	0	0	0	2,5	0	5	-	-	-	-	-----	1
<i>two</i>	phe-L, leu-L	0	1,5	1	-0,25	1,81	-0,06	6	+	+	+	-	1:3	2
		0	1,5	1	-1,25	1,56	-0,31	7	+	+	-	-	1:3	2
	leu-L, his-L	0	2	1	-1,67	2,33	-0,42	8,67	-	-	-	+	2:1	2
	leu-L, histsd	0	1,33	1	-0,67	1,42	-0,17	8,67	-	-	-	-	2:1	2
	lys-L, his-L	0	1,5	2	-2,5	0,5	-0,63	9,5	-	-	-	+	1:1	1
	val-L, his-L	0	0,67	1	-1	0,17	-0,25	8	-	-	-	+	2:1	2



727 **Figure 1: Metabolic complementations suggested by the *iJC86* model.**



730 **Figure 2: Representation of the energetics of *Portiera* according to the *i*JC86 model.**



732

733

734

735

736

737

738

739

740

741

742

743 **Figure 3: Graph representing the coupling between phenylalanine and tryptophan**  
 744 **biosynthesis in *iJC86* model of *P. aleyrodidarum* metabolism if D-ribulose-5-phosphate-3-**  
 745 **epimerase and D-glucose-6-phosphate isomerase are not included as orphan.**

746

747

748

749

750

751

752

753

754

755

756

757

758

759

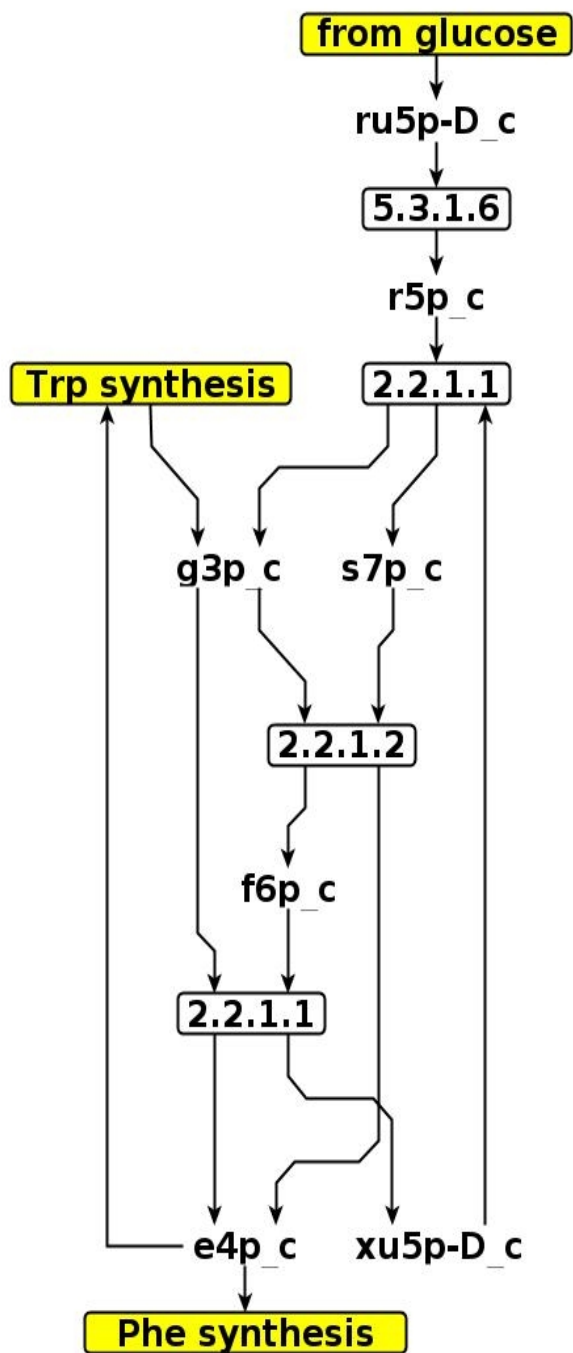
760

761

762

763

764



765 **Figure 4: Impact of  $\beta$ -carotene synthesis on the metabolic performance of the *iJC86* model of**  
766 ***Portiera's* metabolism.**

